Hot deformation characteristics and dynamic recrystallization behaviors of adamite cast steel for work rolls in hot rolling

Y-J. An, K-T. Cho, J-Y. Jeon, S-E. Shin, D-G. Kim

Hot workability and dynamic recrystallization(DRX) behavior of adamite cast steel used as work rolls for hot rolling were investigated in order to improve the service life through hot forging. The specimens were heated at the two different initial heating temperatures(IHT) of 1200 °C or 1100 °C. And the hot compression tests(HCT) were performed in temperature ranges from 1100 to 800 °C with the strain rate ranges from 1.0 to 0.001 s^{-1}. In the processing maps, the stable hot working regions with η values as 31-24 % and positive ξ in the IHT of 1100 °C are larger than that of 1200 °C. In DRX behavior, the DRX fractions(f_{DRX}) are higher than 50 % in all hot compressed specimens with the IHT of 1100 °C compared to the IHT of 1200 °C. The defects such as partial meltings or cracks at the HCT temperature of 1100 °C or 800 °C are observed in both the IHTs of 1200 °C and 1100 °C. However, the defects observed at the IHT of 1100 °C are significantly alleviated compared to the IHT of 1200 °C.

KEYWORDS: ADAMITE, PROCESSING MAP, MICROSTRUCTURE, RECRYSTALLIZATION, WORK ROLL

INTRODUCTION

Adamite with a carbon content of 1.4 to 2.0 wt. % manufactured by the casting is used as work rolls for hot rolling [1]. Nowadays, rolling conditions are becoming harsh since steel makers increase rolling productivity with demand for high strength steels. So that it causes fatigue cracks and spalling on the surfaces of work rolls [2,3]. Therefore, the decreased service life of work rolls leads to an increase in the replacement cost of work rolls and a decrease in rolling productivity. In recent, the studies are reported on reducing the casting defects and improving mechanical properties such as wear resistance and fatigue resistance by applying hot forging to adamite cast roll [4,5]. However, high carbon steels are limited in application of hot forging due to its narrow hot forging regions and precipitation of cementites resulting in brittleness [6]. Therefore, the objective of this study is to derive applicability of hot forging on adamite cast steel with a carbon content of 1.6 wt. % through the HCT and DRX behavior.

Experimental material and procedure

The materials used were prepared from adamite cast roll

Yu-Jeong An
Purpose Built Mobility Group, Seonam Technology Application Division, Korea Institute of Industrial Technology, Republic of Korea; Department of Materials Science and Metallurgical Engineering, Sunchon National University, Republic of Korea

Kyun-Taek Cho, Jae-Yeol Jeon
Purpose Built Mobility Group, Seonam Technology Application Division, Korea Institute of Industrial Technology, Republic of Korea

Se-Eun Shin
Department of Materials Science and Metallurgical Engineering, Sunchon National University, Republic of Korea

Dae-Geun Kim
Materials Science and Chemical Engineering Center, Institute for Advanced Engineering, Republic of Korea

and the chemical composition is given in Tab. 1. The HCT for deriving the processing map to evaluate hot workability was carried out by gleeble thermal-mechanical simulator. The test specimens were machined with a diameter of 10 mm and with a height of 12 mm. In the HCT, the initial heating was performed at the two different test temperatures of 1200 °C or 1100 °C with a heating rate of 4 °C/s to evaluate the effect of the IHT on hot workability. And then, all specimens were rapidly cooled to the HCT temperatures of 1100 °C, 1000 °C, 900 °C, and 800 °C with the strain rates of 1.0 s^{-1}, 0.1 s^{-1}, 0.01 s^{-1}, and 0.001 s^{-1}, respectively. All specimens were compressed to 50 % in height ($\Delta h/h_0$). The processing maps were obtained by using flow stress-strain curves from the HCT and the microstructures were analyzed by field emission scanning electron microscopy(FE-SEM) to confirm the reliability of the obtained processing maps. The DRXed behaviors were analyzed by electron backscatter diffraction(EBSD).

Tab.1 - Chemical compositions of adamite.

Chemical compositions of adamite							
	C	Si	Mn	Cr	Mo	P	S
Spec	1.4~2.0	0.3~0.7	0.5~1.0	0.8~1.6	0.2~0.5	~0.035	~0.030
Results	1.58	0.36	0.79	1.08	0.25	0.035	0.004

RESULTS

Flow stress-strain curves

Flow stress-strain curves obtained at the HCT temperature ranges from 1100 to 800 °C with the strain rate ranges from 1.0 to 0.001 s^{-1} with the two different IHTs are shown in Fig. 1. Flow stress-strain curves in Fig. 1(a) and (b) exhibit work hardening up to 0.2 % offset yield point regardless of the strain rates and the HCT temperatures followed by gradually softening to the true strain of 0.69. It means that softening occurs due to the DRX. In general, flow stresses decrease as the HCT temperature increases and the strain rate decreases. In com-pared to the flow stresses and the critical strains at the IHTs of 1200 °C and 1100 °C, the flow stresses and the critical strains at the IHT of 1100 °C are lower than that of the IHT of 1200 °C. This may imply that the DRX at the IHT of 1100 °C is well developed than that of the IHT of 1200 °C.

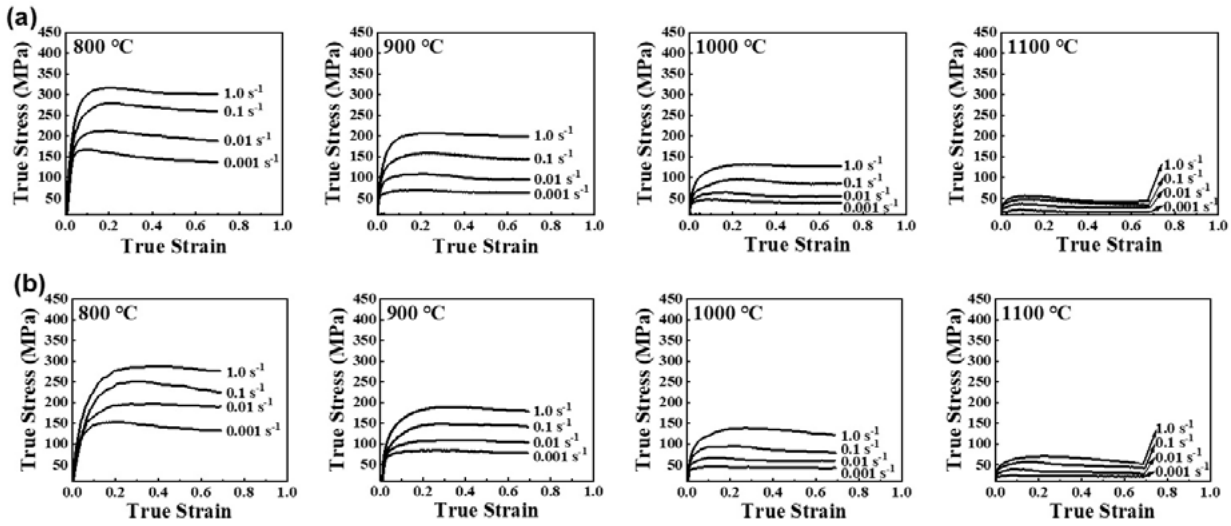

Fig.1 - Flow stress-strain curves of (a) the IHT of 1200 °C and (b) the IHT of 1100 °C.

Processing map

The processing maps of adamite cast steel are shown in Fig. 2 and the parameters of the processing map as the power dissipation efficiency and the instability are as below in Eq. (1) and Eq. (2) [7,8].

$$\eta = \frac{J}{J_{max}} = \frac{2m}{m+1} \quad [1]$$

$$\xi(\dot{\varepsilon}) = \frac{\partial \ln [m/(m+1)]}{\partial \ln \dot{\varepsilon}} + m < 0 \quad [2]$$

In the processing map of the IHT of 1200 °C, high η values as 28-24 % are shown in the HCT temperature ranges from 1000 to 900 °C with the strain rate ranges from 1.0 to 0.001 s^{-1} as shown in Fig. 2(a). In the processing map of the IHT of 1100 °C, higher η values as 31-24 % are shown compared to the same HCT temperatures with the strain rates in the IHT of 1200 °C. And relatively high η values as 27 % or 22 % are shown in the HCT temperature of 1100 °C or 800 °C with the strain rate of 0.001 s^{-1} different from the IHT of 1200 °C. It would be due to the difference in the microstructures of the hot compressed specimens. In previous studies, DRX occurs at η values as 32-22 % in a high carbon steel with 1.2 wt. % C [9]. It means that DRX would occur in both the above high η regions in the obtained processing maps. And also, it is thought that η values less than 22 % with negative ξ would be unstable regions in Fig. 2(a) and (b).

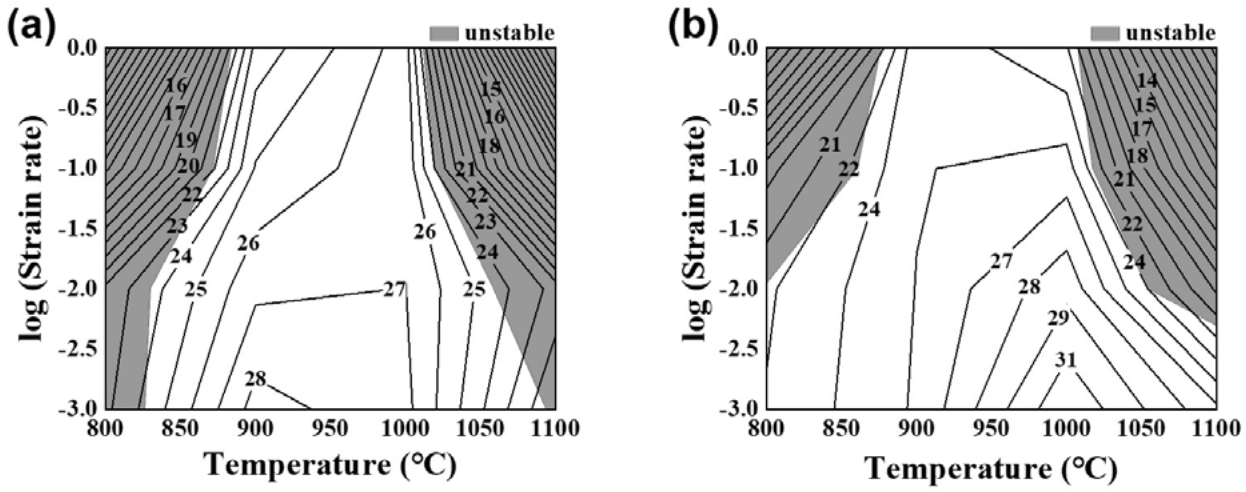

Fig.2 - Flow stress-strain curves of (a) the IHT of 1200 °C and (b) the IHT of 1100 °C.

Microstructural analysis

To confirm the reliability of the obtained the processing maps, the microstructures of the bulged side surface of the hot compressed specimens are shown in Fig. 3. In the microstructures of the hot compressed specimens with the IHT of 1200 °C, partial meltings or cracks at cementites are found at HCT temperature of 1100 °C or 800 °C regardless of the strain rates. On the other hand, partial meltings or cracks are not found at HCT temperature ranges from 1000 to 900 °C regardless of the strain rates. In the microstructures of the hot compressed specimens with the IHT of 1100 °C, partial meltings or cracks are found at HCT temperature of 1100 °C or 800 °C at the strain rate ranges from 1.0 to 0.01 s^{-1}. On the other hand, partial meltings or cracks are not found at HCT temperature ranges from 1000 to 900 °C regardless of

the strain rates as shown in Fig. 3(a). The hot compressed specimens with the defects show negative ξ with η less than 22 % in the processing maps as shown in Fig. 2(a) and (b). The number and size of the defects in the hot compressed specimens with the IHT of 1100 °C decrease and are milder than that of the IHT of 1200 °C. The results of microstructure observations according to the IHTs and the HCT conditions such as temperatures and strain rates correspond well with the obtained the processing maps. The reasons of partial meltings or cracks will be discussed in 3.1.

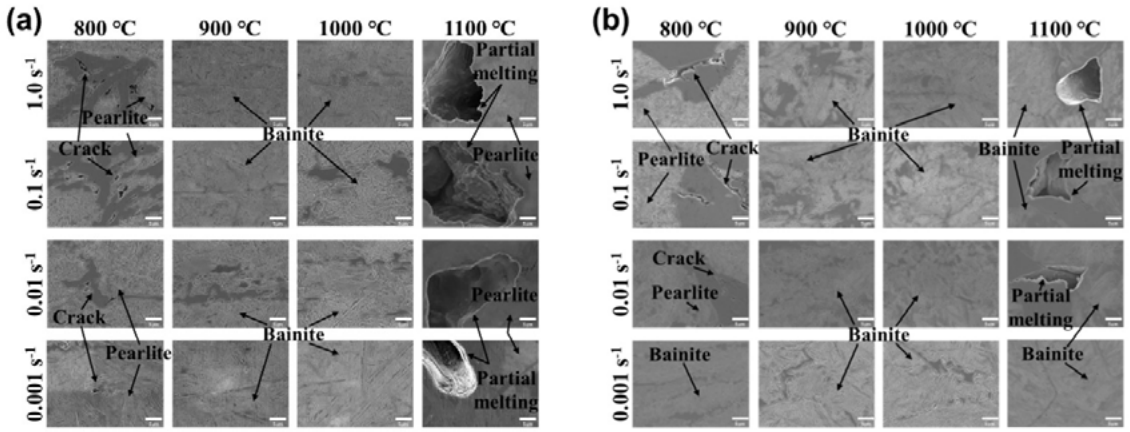

Fig.3 - FE-SEM images of the hot compressed specimens after (a) the IHT of 1200 °C and (b) the IHT of 1100 °C.

DRX behaviors

The DRX behaviors of the hot compressed specimens at the HCT temperature ranges from 1100 to 800 °C with the strain rate of 1.0 s^{-1} or 0.001 s^{-1} according to the IHTs were analyzed by EBSD. The f_DRX calculated by considering the regions with GOS ≤ 2˚ as DRXed grain using grain orientation spread(GOS) are shown in Fig. 4. In general, partially DRX is known to occur when f_{DRX} is higher than 50 % [10]. In the IHT of 1200 °C, partially DRX as f_{DRX} higher than 50 % occurs in the HCT temperature ranges from 1000 to 900 °C with the strain rate of 1.0 s-1 or 0.001 s^{-1}. However, partially DRX do not occur at the HCT temperature of 1100 °C or 800 °C regardless of the strain rates. In the IHT of 1100 °C, partially DRX occurs in all hot compressed specimens different from Fig. 4(a). And also, f_{DRX} increases as increasing the HCT temperatures. The reason of lower f_{DRX} of the hot compressed specimen at 1100 °C or 800 °C in Fig. 4(a) is that pearlites were mainly observed as shown in Fig. 3. It means that DRX could not be well developed in pearlites due to lower carbon contents [11]. In comparison with the strain rates, as the strain rate is slower, f_{DRX} increases irrespective of the IHT as shown in Fig. 4. Therefore, the DRX behaviors analyzed by EBSD agree with the processing map in Fig. 2.

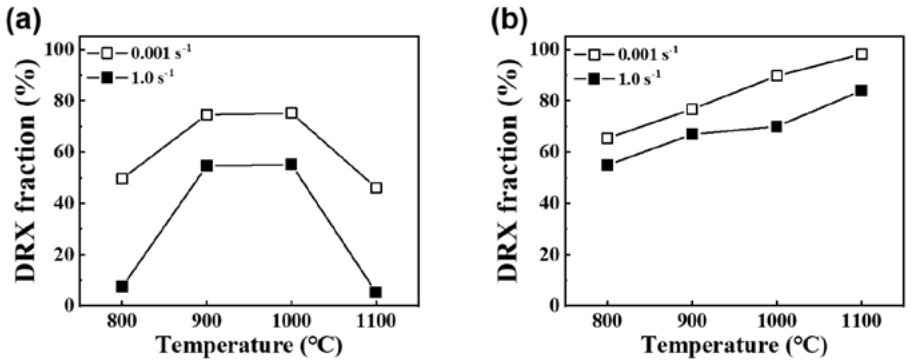

Fig.4 - DRX fractions of the hot compressed specimens with (a) the IHT of 1200 °C and (b) the IHT of 1100 °C.

DISCUSSIONS

The reason of defects

As mentioned earlier in 2.3, partial meltings or cracks at cementites are observed in the hot compressed specimen at 1100 °C or 800 °C with the IHT of 1200 °C or 1100 °C. In order to reveal the reason of partial meltings at first, the specimens were heated to 1200 °C or 1100 °C, respectively and then held for 5 minutes at each of the individual temperatures without the HCT. The microstructures of each heat-treated specimens are shown in Fig. 5. Partial meltings or marks of partial melting are observed together in the specimen heat-treated at 1200 °C and marks of partial melting are only observed in the specimen heat-treated at 1100 °C as shown in Fig. 5. It is thought that the heating temperature higher than 1100 °C would touch the mushy zone of adamite with a carbon content of 1.6 wt. %. Therefore, partial meltings or marks of partial melting are not probably solidified or probably still exist in the specimens during the HCT after the initial heating at 1200 °C even rapidly cooled to 1100 °C. Also, the authors thought that the solidus temperature of cementites is relatively lower because of segregation of carbon atoms [12]. So that partial meltings are observed in the hot compressed specimens at 1100 °C after the initial heating at 1100 °C. And the reason of cracks in the hot compressed specimens at 800 °C regardless of the IHTs is thought to be the strength difference between cementites and the matrix [13]. Consequently, the authors propose that the appropriate heating temperature of adamite for hot working without the defects such as partial meltings is supposed to be less than 1100 °C.

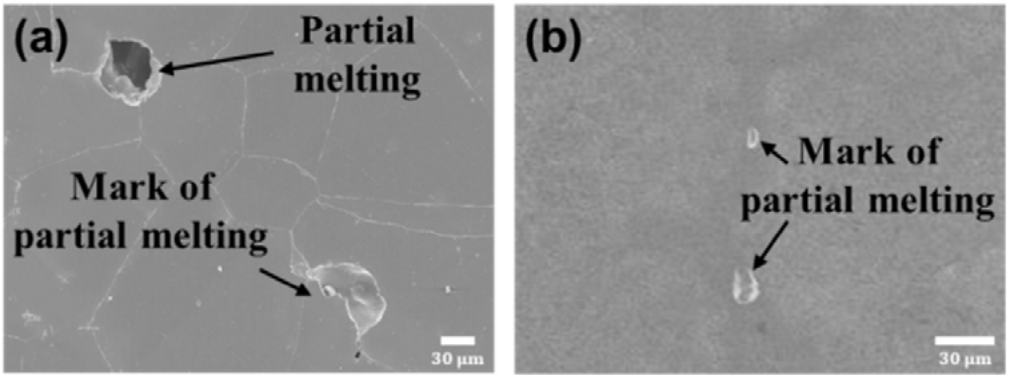

Fig.5 - FE-SEM images of the heat-treated specimens at (a) 1200 °C and (b) 1100 °C.

CONCLUSIONS

The HCT was carried out on adamite cast steel to derive applicability of hot forging. Hence, the hot workability and the DRX behavior were evaluated. The following remarks can be drawn from this study:

(1) The stable hot working regions with η values as 31-24 % and positive ξ in the processing map with the IHT of 1100 °C are largely obtained compared to the IHT of 1200 °C.

(2) The f_{DRX} higher than 50 % in the hot compressed specimens after the IHT of 1100 °C are higher than that of the IHT of 1200 °C and the slower strain rates increase the f_{DRX} in both. Also, relatively lower f_{DRX}s in the HCT temperature of 1100 °C or 800 °C after the IHT of 1200 °C are related to pearlites with relatively lower carbon contents.

(3) The defects such as partial meltings or cracks are observed in the hot compressed specimen at 1100 °C or 800 °C after the IHT of 1200 °C or 1100 °C. However, the number and size of the defects in the hot compressed specimens with the IHT of 1100 °C decrease and are milder than that of the IHT of 1200 °C.

REFERENCES

[1] Kiss, I, Alexa, V, Serban, S. et al., Statistical research using the multiple regression analysis in areas of the cast hypereutectoid steel rolls manufacturing, IOP Conference Series: Materials Science and Engineering, 2018;294:1757-899X.
[2] Ringsberg, Jonas W, Life prediction of rolling contact fatigue crack initiation, International Journal of fatigue, 2001;23:575-586.
[3] Qiong, Wu, Da-le, Sun, Chang-sheng, Liu, Chun-guang, Li, Analysis of surface and sub-surface initiated spalling of forged cold work rolls, Engineering Failure Analysis, 2008;15:401-410.
[4] SUZUKI, Akio, Recent Progress in the Rolling Mills-Part II, Transactions of the Iron and Steel Institute of Japan, 1984;24:308-329.
[5] NOGUCHI, Hiroshi, HIRAOKA, Hisashi, WATANABE, Yasuo, SAYAMA, Yasuhiro, Hardness and wear resistance of adamite for work rolls in hot rolling mill, Transactions of the Iron and Steel Institute of Japan, 1988;28:478-484.
[6] McQueen, HJ, Imbert, CAC, Sherby, Oleg D, Hot deformation of hypereutectoid steels, Materials Science Forum, 2003;426:865-870.
[7] Prasad, YVRK, Processing maps: A status report, Journal of Materials Engineering and Performance, 2003;12:638-645.
[8] Ziegler, H, Some extremum principles in irreversible thermodynamics, with application to continuum mechanics Progress in Solid Mechanics, Sneddon, and Hill, 1963;4:93-193.
[9] Prasad, YVRK, Rao, KP, Sasidhar, S, Hot working guide: a compendium of processing maps, ASM international, 2015;249-250.
[10] Humphreys, Frederick John, Hatherly, Max, Recrystallization and related annealing phenomena, 2012.
[11] Zhao, Haitao, Qi, Jianjun, Liu, Guoquan et al., A comparative study on hot deformation behaviours of low-carbon and medium-carbon vanadium microalloyed steels, Journal of Materials Research and Technology, 2020;9:11319-11331.
[12] Jeon, Jae-Yeol, Matsumoto, Ryo, Utsunomiya, Hiroshi, Die quenching limit of AA2024 aluminum alloy billet on servo press, Journal of Materials Processing Technology, 2014;214:2514-2521.
[13] Ungár, T, Dragomir, I, Révész, Á, Borbély, A, The contrast factors of dislocations in cubic crystals: the dislocation model of strain anisotropy in practice, Journal of applied crystallography, 1999;32:992-1002.
[24] Li CX, Georges J, Li XY. Active screen plasma nitriding of austenitic stainless steel. Surface Engineering 2002;18(6):453–7.
[25] Georges J. Nitriding process and nitriding furnace therefor, US Patent (US 5,989,363); 1999.
[26] Burlacov I, Hamann S, Spies H-J, Dalke A, Röpcke J, Biermann H. A Novel Approach of Plasma Nitrocarburizing Using a Solid Carbon Active Screen – a Proof of Concept. HTM Journal of Heat Treatment and Materials 2017;72(5):254–9.
[27] Jacob W, Hopf C, Schlüter M. Chemical sputtering of carbon by nitrogen ions. Appl. Phys. Lett. 2005;86(20):204103.
[28] Schlüter M, Hopf C, Jacob W. Chemical sputtering of carbon by combined exposure to nitrogen ions and atomic hydrogen. New Journal of Physics 2008;10(5):53037.
[29] Jafarpour SM, Pipa AV, Puth A, Dalke A, Röpcke J, van Helden J-PH et al. Effects of Plasma-Chemical Composition on AISI 316L Surface Modification by Active Screen Nitrocarburizing Using Gaseous and Solid Carbon Precursors. Metals 2021;11(9):1411.
[30] Dalke A, Burlacov I, Hamann S, Puth A, Böcker J, Spies H-J et al. Solid carbon active screen plasma nitrocarburizing of AISI 316L stainless steel: Influence of N_2-H_2 gas composition on structure and properties of expanded austenite. Surface and Coatings Technology 2019;357:1060–8.
[31] Puth A, Kusýn L, Pipa AV, Burlacov I, Dalke A, Hamann S et al. Spectroscopic study of plasma nitrocarburizing processes with an industrial-scale carbon active screen. Plasma Sources Sci. Technol. 2020;29(3):35001.
[32] Gordon IE, Rothman LS, Hargreaves RJ, Hashemi R, Karlovets EV, Skinner FM et al. The HITRAN2020 molecular spectroscopic database. Journal of Quantitative Spectroscopy and Radiative Transfer 2022;277:107949.

TORNA ALL'INDICE >